European Journal of Medicinal Chemistry 45 (2010) 5183–5199

Contents lists available at ScienceDirect

European Journal of Medicinal Chemistry

journal homepage: http://www.elsevier.com/locate/ejmech

Original article

QSAR modeling, synthesis and bioassay of diverse leukemia RPMI-8226 cell line active agents

Alan R. Katritzky [a,*], Adel S. Girgis [a,b], Svetoslav Slavov [a], Srinivasa R. Tala [a], Iva Stoyanova-Slavova [a]

[a] Center for Heterocyclic Compounds, University of Florida, Department of Chemistry, Gainesville, FL 32611-7200, United States
[b] Pesticide Chemistry Department, National Research Centre, Dokki, 12622 Cairo, Egypt

ARTICLE INFO

Article history:
Received 18 June 2010
Received in revised form
6 August 2010
Accepted 10 August 2010
Available online 19 August 2010

Keywords:
Leukemia RPMI-8226 cell line
Anti-tumor agents
Bis(oxy)bis-urea derivatives
Bis(sulfanediyl)bis-urea derivatives
QSAR
CODESSA PRO

ABSTRACT

A rigorous QSAR modeling procedure employing CODESSA PRO descriptors has been utilized for the prediction of more efficient anti-leukemia agents. Experimental data concerning the effect on leukemia RPMI-8226 cell line tumor growth of 34 compounds (treated at a dose of 10 μM) was related to their chemical structures by a 4-descriptor QSAR model. Four bis(oxy)bis-urea and bis(sulfanediyl)bis-urea derivatives (**4a**, **4b**, **8**, **11a**) predicted as active by this model, together with **11b** predicted to be of low activity, were synthesized and screened for anti-tumor activity utilizing 55 different tumor cell lines. Compounds **8** and **11a** showed anti-tumor properties against most of the adopted cell lines with growth inhibition exceeding 50%. The highly promising preliminary anti-tumor properties of compounds **8** and **11a**, were screened at serial dilutions (10^{-4}–10^{-8} μM) for determination of their GI_{50} and TGI against the screened human tumor cell lines. Compound **11a** ($GI_{50} = 1.55$, TGI = 8.68 μM) is more effective than compound **8** ($GI_{50} = 58.30$, TGI = >100 μM) against the target leukemia RPMI-8226 cell line. Compound **11a** also exhibits highly pronounced anti-tumor properties against NCI-H226, NCI-H23 (non-small cell lung cancer), COLO 205 (colon cancer), SNB-75 (CNS cancer), OVCAR-3, SK-OV-3 (ovarian cancer), A498 (renal cancer) MDA-MB-231/ATCC and MDA-MB-468 (breast cancer) cell lines ($GI_{50} = 1.95$, 1.61, 1.38, 1.56, 1.30, 1.98, 1.18, 1.85, 1.08, TGI = 8.35, 6.01, 2.67, 8.59, 4.01, 7.01, 5.62, 6.38, 5.63 μM, respectively). Thus **11a** could be a suitable lead towards the design of broad spectrum anti-tumor active agents targeting various human tumor cell lines.

1. Introduction

Cancer is a leading cause of death world wide. Despite technological advances, the index of cancer cure remains low and its treatment is a challenge. The childhood cancer Leukemia affects a significant segment of the population, with 26% of all cases and 30% mortality [1]. While the incidence of leukemia has remained relatively unchanged, its treatment has made progress and since 1950, mortality rates for childhood cancer declined by more than 50%. In 1960, few could survive acute lymphoid "childhood leukemia" while now 86% of children and teens so diagnosed are still alive 5 years later [2,3]. The overall five-year (1995–2001) survival rate for acute myeloid leukemia has also increased from 38% to 65% [4]. Despite the success of clinical trials, new agents and treatments have limitations related to their side effects and the development of acquired drug resistance [5]. Active new therapeutic agents with novel modes of action and fewer side effects are still needed [6].

A wide range of QSAR[1] tools for modeling has been developed during the past three decades; our group has utilized CODESSA PRO[2] [7] which calculates numerous quantitative descriptors using information extracted from the molecular structure. CODESSA PRO has successfully correlated and predicted diverse physicochemical and biological properties [8–11]. The present study reports the QSAR modeling of biological data obtained at the National Cancer Institute, Bethesda, USA using the leukemia RPMI-8226 cell line according to standard procedures [12–17a]. Based on the QSAR study we predicted new molecules expected to be bio-active, and synthesized representative examples. The training dataset adopted herein the present study includes many types of chemical structures (Table 1), thus diversity of pharmacological modes of action is expected. Many of the compounds in the training dataset, especially the nicotinamide derivatives (compounds **14**–**24**, Table 1) are

* Corresponding author. Tel.: +1 352 392 0554; fax: +1 352 392 9199.
E-mail address: katritzky@chem.ufl.edu (A.R. Katritzky).

[1] Quantitative Structure–Activity Relationship.
[2] COmprehensive DEscriptors for Structural and Statistical Analysis.

0223-5234/$ – see front matter © 2010 Elsevier Masson SAS. All rights reserved.
doi:10.1016/j.ejmech.2010.08.033

closely structurally related to potent inducers of apoptosis agents such as *N*-(4-methoxy-2-nitrophenyl)pyridine-3-carboxamide ($EC_{50} = 1.6$, 0.88, 2.9 μM in the caspase activation assay in human breast cancer T47D, ZR75-1 and colorectal DLD-1 cell lines, respectively) and 6-methyl-*N*-(4-ethoxy-2-nitrophenyl)pyridine-3-carboxamide ($EC_{50} = 0.082$, 0.052, 0.11 μM in the caspase activation assay in human breast cancer T47D, ZR75-1 and colorectal DLD-1 cell lines, respectively) [17b]. However, the present work is focused on the preparation and anti-tumor bioactivity screening of compounds predicted from a QSAR model and presented as a medicinal chemistry study targeting the discovery of anti-tumor active hits.

2. Dataset

Percentage growth of the tumor "leukemia RBMI-8226 cell line" treated at a dose of 10 μM with the 34 compounds tested was measured relative to control experiments (Table 1) [12–14,18].

3. Methodology

Compound structures were drawn using ChemDraw Ultra 11.0 [19] and each structure was further optimized by the following procedure:

i) conformational search analysis utilizing the "random walk" method as implemented in HyperChem v. 7.5 [20] was used to identify the lowest energy conformer;
ii) in view of the size and complexity of the anti-leukemia agents studied, the lowest energy conformation obtained in step "i" was subjected to a preliminary optimization with molecular mechanics force field (MM+);
iii) the AM1 [21] semi-empirical method using an RMS gradient of 0.05 kcal/mol was then applied to obtain the final geometries of the compounds for export to CODESSA PRO software as the next step.

More than 500 constitutional, topological, geometrical, quantum chemical and electrostatic descriptors were calculated with the CODESSA PRO software package. The LogP descriptor was also calculated and added to the set of CODESSA descriptors as an important transportation limiting factor. The optimal descriptor subset was then selected by the BMLR[3] [22a] algorithm based on the selection of orthogonal descriptor pairs.

4. Multi-linear modeling

4.1. Data distribution and transformation of the original property

To improve the distribution of the experimental data, transformations of the percentage inhibition of the tumor relative to control experiments were performed. The logarithmic transformation was found to produce a data distribution close to normal (Fig. 1) and was thus preferred to alternative transformations involving reciprocal, logarithmic reciprocal and squared functions. One compound (ID #25), which is in fact one of the two singletons in the dataset, disturbed slightly the normal distribution of the data causing a long left branch of the probability density function. However, this compound fits well the general QSAR relationship carried out in Table 2, and was retained in the model.

5. Results and discussion

The original dataset of 34 compounds comprises 5 structurally distinct subsets containing respectively ten (**1**–**10**), three (**11**–**13**), eleven (**14**–**24**), two (**27**–**28**) and six (**29**–**34**) compounds, together with two singletons **25** and **26**. The heterogeneity of the dataset of 34 compounds and the need to select a robust test set representative of the general population, led us to the following procedure: i) for each of the three bigger subsets (**1**–**10**; **14**–**24**; **29**–**34**) the average anti-tumor activity was found and the member of each subset characterized with an activity closest to the average (i.e., compounds **1**, **17** and **29** respectively) was moved to the test set; ii) to estimate the ability of the model to predict the activity of structurally diverse compounds the small subset of three compounds (**11**–**13**) and both the singletons (**25** and **26**) were also moved to the test set. Thus, a training set of 26 compounds and an external test set of 8 compounds (approximately 1/4 of the total) were formed, complying with standard QSAR recommendations [22b].

For the next stage, the BMLR stepwise regression algorithm, using subsets of noncollinear descriptors, generated the best *n*-parameter regression equations ($n \geq 2$), based on the highest R^2 and *F* values obtained in the process of calculations. Since, the correlations are not statistically reliable if the variables are mutually intercorrelated, the BMLR rejects the simultaneous use of descriptors with intercorrelation coefficients larger than a certain user defined threshold value (in this case we took $R^2 = 0.5$) (Fig. 2).

QSAR models with up to 6 descriptors were generated (the maximum number allowed according to the 5:1 rule of thumb – the ratio between the data points and the number of descriptors). We considered the statistical parameters including the square of the correlation coefficient (R^2), the cross-validated correlation coefficient (R^2_{cv}), the Fisher criterion (*F*) and the predictive R^2 (R^2_{test}). We then relied on Occam's parsimony principle to select a model with 4 descriptors as optimal (see Table 2).

$N = 26$ (training set); $R^2 = 0.771$; $R^2_{cv} = 0.602$; $R^2_{test} = 0.599$ (for the test set of 8 compounds described above); $F = 17.7$; $s^2 = 0.0376$.

Ranges: Observed (0.780; −2.035). Predicted (0.887; −2.138).

The descriptors of Table 2 can be arranged based on their level of significance ("*t*-criterion") in the following order: "WPSA-3 Weighted PPSA[4] (PPSA3 * TMSA/1000) (MOPAC PC)" > "Maximum resonance energy for bond C–N" > "Principal moment of inertia B" > "HA dependent HDSA-1/TMSA (MOPAC PC) (all)".

The most important descriptor, namely the "WPSA-3 Weighted PPSA" represents the portion of the total molecular surface area which is positively charged. The negative regression coefficient sign of this descriptor suggests that bulky molecules, with the presence of few electronegative atoms such as O, S, Cl, N will be of reduced potency as anticancer agents.

The second descriptor in order of significance is the "Maximum resonance energy for bond C–N". As expected this descriptor has largest values for compounds containing a nitrile group (see ID 25, 27 and 28 in Table 1). The negative regression coefficient of this descriptor implies that the high resonance energy of the C–N bond lowers the anti-tumor activity of compounds containing a nitrile group; this is well illustrated by compounds **25**, **27** and **28** which are among the least active agents with inhibition activities of 0.96, 11.91 and 24.86, respectively.

The "Principal moment of inertia B" is related to the optimal size and shape of the active molecules; molecules of size larger than the optimal may well experience steric hindrance and thus inability to bind efficiently to the target.

[3] Best Multi-Linear Regression.

[4] Partial Positive Surface Area.

Table 1
Structural formulae of the compounds under study and observed and predicted anti-tumor properties.

ID	Chemical structure	Observed % growth of tumor	Observed % growth inhibition of tumor	Log(observed % growth inhibition of tumor)	Log(predicted % growth inhibition of tumor)	Δ(obs. – pred.)
1[a*]	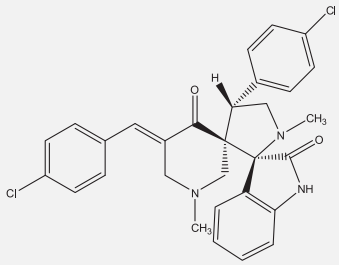	38.54	61.46	1.789	2.104	−0.315
2[a]	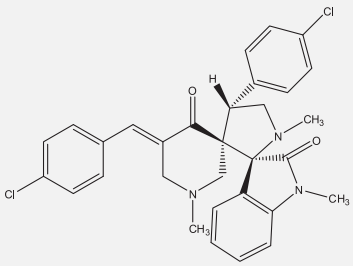	38.04	61.96	1.792	2.138	−0.345
3[a]	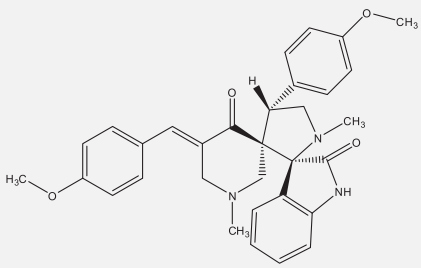	20.74	79.26	1.899	1.966	−0.067
4[a]	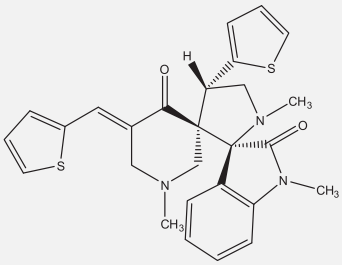	10.58	89.42	1.951	1.702	0.250
5[b]	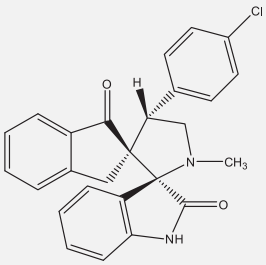	36.59	63.41	1.802	1.750	0.052

(*continued on next page*)

Table 1 (*continued*)

ID	Chemical structure	Observed % growth of tumor	Observed % growth inhibition of tumor	Log(observed % growth inhibition of tumor)	Log(predicted % growth inhibition of tumor)	Δ(obs. – pred.)
6[b]	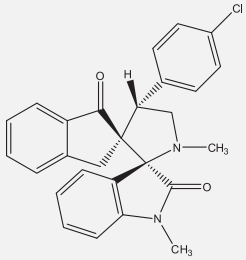	13.37	86.63	1.938	1.785	0.153
7[b]	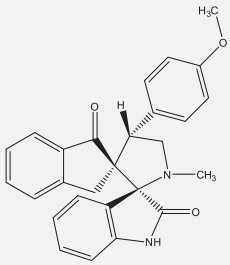	66.75	33.25	1.522	1.761	−0.239
8[b]	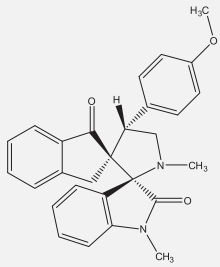	17.73	82.27	1.915	1.795	0.120
9[b]	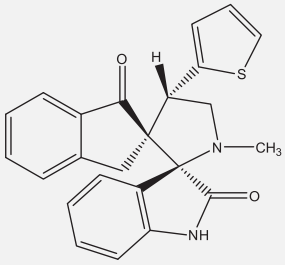	89.11	10.89	1.037	1.164	−0.127
10[b]	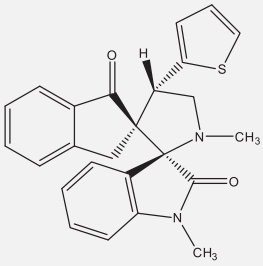	87.94	12.06	1.081	1.168	−0.087

Table 1 (*continued*)

ID	Chemical structure	Observed % growth of tumor	Observed % growth inhibition of tumor	Log(observed % growth inhibition of tumor)	Log(predicted % growth inhibition of tumor)	Δ(obs. – pred.)
11[c*]	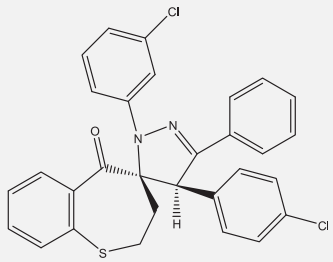	66.79	33.21	1.521	1.417	0.105
12[c*]	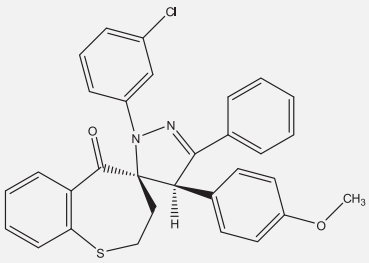	65.71	34.29	1.535	1.416	0.119
13[c*]	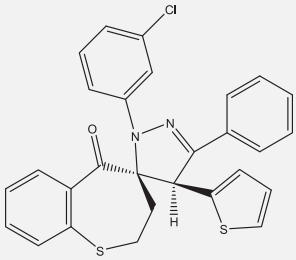	70.18	29.82	1.475	1.176	0.299
14[c]	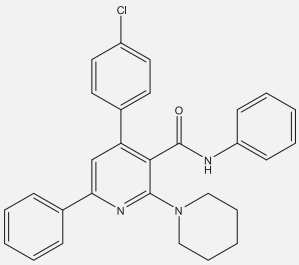	87	13	1.114	1.315	−0.201
15[c]	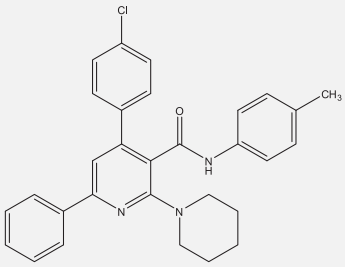	76	24	1.380	1.346	0.035

(*continued on next page*)

Table 1 (*continued*)

ID	Chemical structure	Observed % growth of tumor	Observed % growth inhibition of tumor	Log(observed % growth inhibition of tumor)	Log(predicted % growth inhibition of tumor)	Δ(obs. – pred.)
16[c]	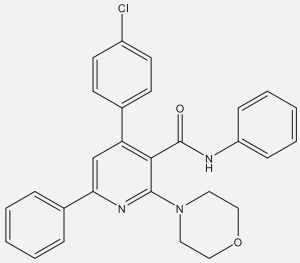	49	51	1.708	1.615	0.093
17[c*]	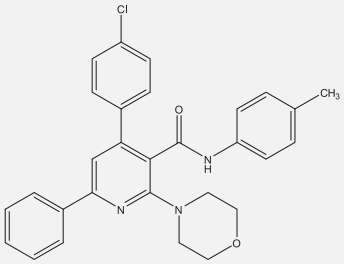	61	39	1.591	1.620	−0.029
18[c]	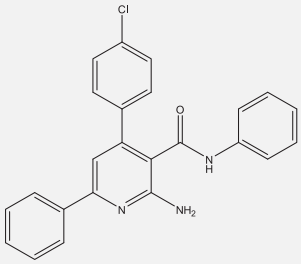	54	46	1.663	1.544	0.119
19[c]	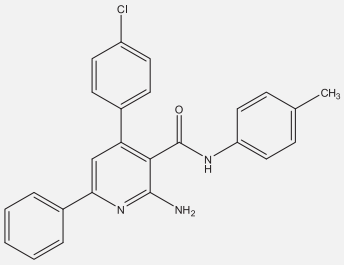	29	71	1.851	1.677	0.174
20[c]	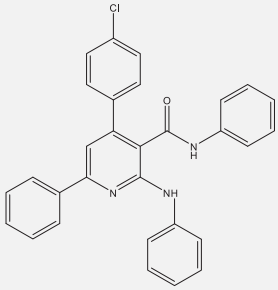	85	15	1.176	1.267	−0.091

Table 1 (*continued*)

ID	Chemical structure	Observed % growth of tumor	Observed % growth inhibition of tumor	Log(observed % growth inhibition of tumor)	Log(predicted % growth inhibition of tumor)	Δ(obs. – pred.)
21[c]	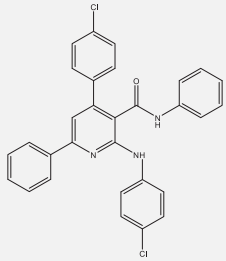	47	53	1.724	1.485	0.239
22[c]	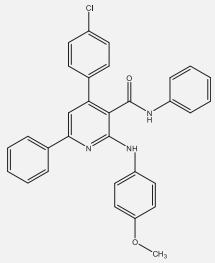	70	30	1.477	1.606	−0.129
23[c]	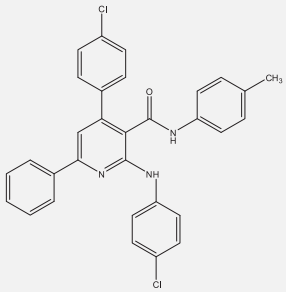	42	58	1.763	1.812	−0.049
24[c]	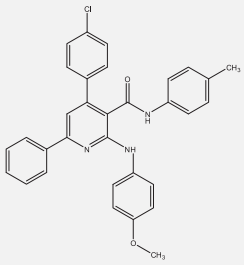	21	79	1.898	1.642	0.256
25[c*]	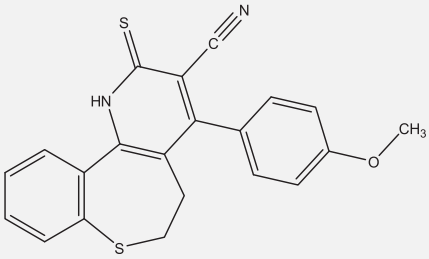	99.04	0.96	−0.018	0.336	−0.353

(*continued on next page*)

Table 1 (*continued*)

ID	Chemical structure	Observed % growth of tumor	Observed % growth inhibition of tumor	Log(observed % growth inhibition of tumor)	Log(predicted % growth inhibition of tumor)	Δ(obs. – pred.)
26[c*]	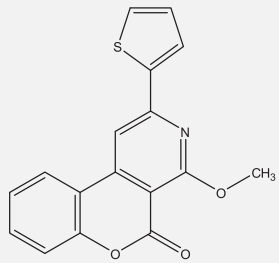	90.89	9.11	0.960	1.078	−0.119
27[c]	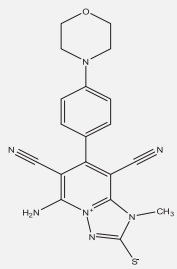	88.09	11.91	1.076	1.290	−0.214
28[c]	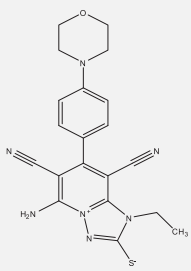	75.14	24.86	1.396	1.242	0.154
29[c*]	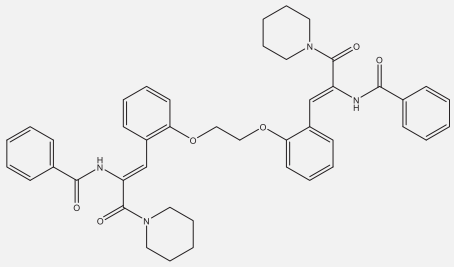	81.67	18.33	1.263	0.871	0.392
30[c]	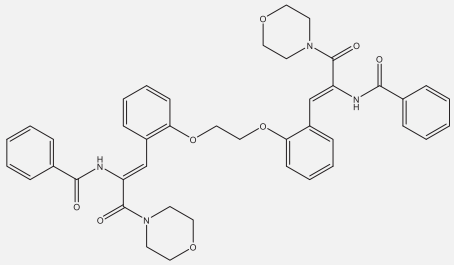	90.85	9.15	0.961	1.253	−0.291

Table 1 (*continued*)

ID	Chemical structure	Observed % growth of tumor	Observed % growth inhibition of tumor	Log(observed % growth inhibition of tumor)	Log(predicted % growth inhibition of tumor)	Δ(obs. – pred.)
31[c]	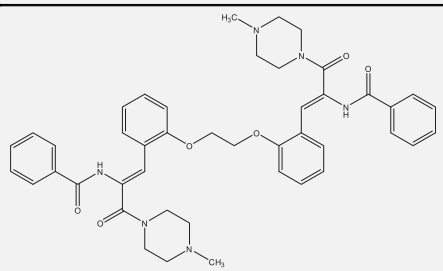	85.26	14.74	1.169	0.900	0.268
32[c]	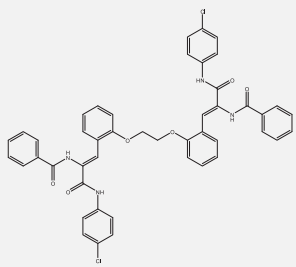	93.97	6.03	0.780	0.888	−0.108
33[c]	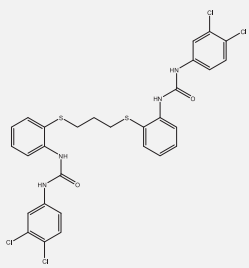	−8.45	108.45	2.035	2.007	0.029
34[c]	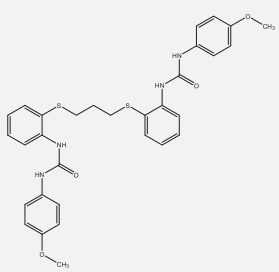	45.39	54.61	1.737	1.733	0.004

The compounds marked with an asterisk are part of the test set.
[a] Ref. [14].
[b] Ref. [12].
[c] Ref. [18].

As the magnitude of the "HA dependent HDSA-1/TMSA (MOPAC PC) (all)" descriptor increases, so does the observed anti-leukemia activity. This descriptor is an indicator for the ability of a molecule to participate in a hydrogen bond formation. Ligand–receptor interactions are generally donor–acceptor based with no covalent bonds formed. This is consistent with the positive regression coefficient of this descriptor.

As emphasized above, the limited size of our dataset requires extensive internal and external validation to prove the stability and to estimate the "true" predictive power of the model. In addition to crossvalidation and external validation we therefore also applied a scrambling procedure to the model. To examine the sensitivity of the proposed QSAR to chance correlations we fitted the model to randomly reordered activity values and then comparing the statistical parameters with those obtained for the actual activities. [23] Twenty such randomizations, produced on average $R^2 = 0.413$ (ranging 0.361–0.472). The substantial difference between the actual R^2 of 0.771 and the averaged R^2 from the scrambling procedure indicates the stability of the model.

6. Chemistry

Based on the model of Table 2, we predicted the activity of some 30 bis-urea containing-compounds similar in structure to the most

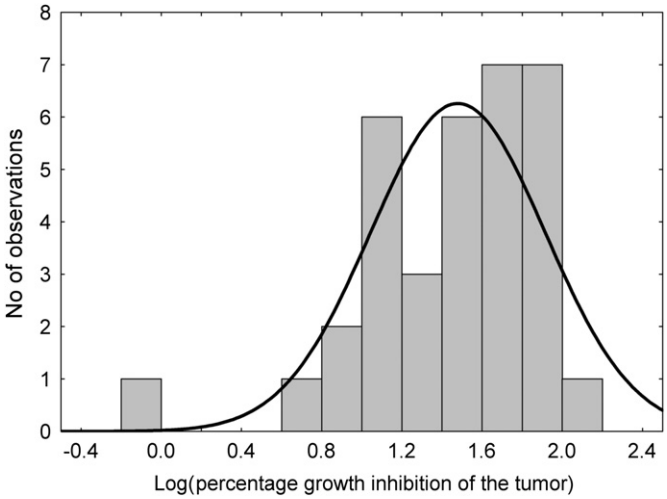

Fig. 1. Probability density function of the logarithmic percentage tumor growth inhibition for the studied set of 34 compounds.

active one (compound #**33** in Table 1). We selected five of these (**4a**, **4b**, **8**, **11a** and **11b**) in order to provide a measure of the predictive power of our model: four of these were selected from among these predicted as most active and one of low predicted activity was also picked. The predicted percentages of tumor growth inhibition were: **4a** – 109.7, **4b** – 61.6, **8** – 94.2, **11a** – 59.7 (high activity) and **11b** – 36.7 (low activity). As described below compounds **4a**, **4b**, **8**, **11a**, and **11b** were synthesized and their anti-tumor activity screened through the Developmental Therapeutics Program of National Cancer Institute, Bethesda, USA.

Schemes 1–3 outline the routes used for synthesis of target compounds **4a**, **4b**, **8**, **11a**, and **11b**. Reaction of the potassium salts of acetamidophenols **1** and **5** with 1,3-dibromopropane in refluxing DMF afforded diacetamide derivatives **2** and **6** respectively. Treatment of **2** and **6** with conc. HCl in refluxing ethanol gave the diamino analogues **3** and **7** respectively; which on reaction with the appropriate isocyanate in dry tetrahydrofuran at room temperature yielded the bis-ureas **4a**,**b** and **8** in 89–93% yield (Schemes 1 and 2).

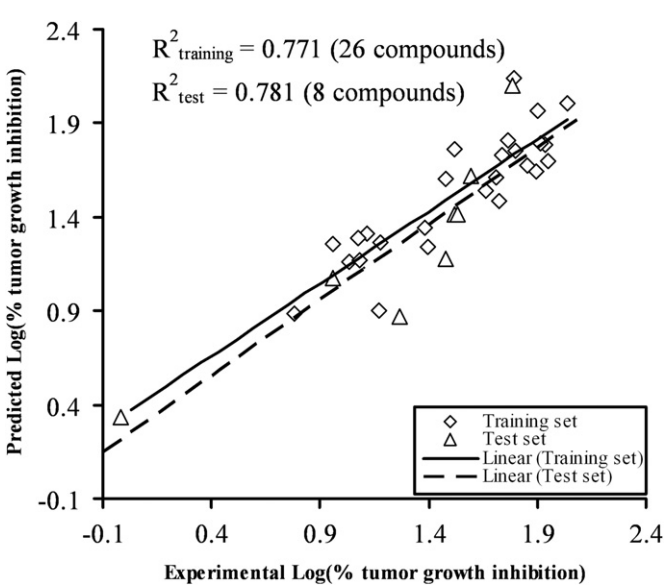

Fig. 2. Predicted vs experimental Log(percentage of tumor growth inhibition).

Table 2
Best 4-descriptor QSAR model.

ID	X	ΔX	t	Descriptor name
0	5.117	0.4471	11.45	Intercept
1	−0.02310	0.002899	−7.970	WPSA-3 Weighted PPSA (PPSA3*TMSA/1000) (MOPAC PC)
2	−0.09639	0.01437	−6.709	Maximum resonance energy for bond C-N
3	−353.7	56.32	−6.281	Principal moment of inertia B
4	3.834	0.8610	4.453	HA dependent HDSA-1/TMSA (MOPAC PC) (all)

Alkylation of 2-aminothiophenol **9** with 1,4-dibromobutane in refluxing ethanol gave diamine dihydrochloride **10** (Scheme 3). Bis-ureas **11a,b** (68–75%) were obtained by reaction of isocyanates and diamine dihydrochloride **10** in dry THF.

7. Anti-tumor activity screening

Compounds (**4a**,**b**; **8**; **11a**,**b**) were screened for anti-tumor activity at a dose of 10 μM utilizing human tumor cell lines, representing leukemia, melanoma and cancers of the lung, colon, brain, ovary, breast, prostate and kidney. Adriamycin was used as a reference standard according to the previously reported standard procedure. [12–17] The results obtained (Table 3) represent percentage growth of the tumor cell lines treated with compounds under investigation relative to control cell experiments. The data obtained revealed that compounds **8** and **11a** showed promising anti-tumor properties against most of the adopted cell lines, whereas compounds **4a**,**b** and **11b** revealed little significant effect (considering >50% inhibition at 10 μM as noticeable activity). Highly active compounds **8** and **11a** were screened at serial dilutions (10^{-4}–10^{-8} μM) to determine GI_{50} (the concentration resulting in a 50% growth inhibition of the tumor compared with the control experiments) and TGI (the concentration resulting in a 100% growth inhibition of the tumor compared with the control experiments). The data obtained (Table 4) indicate that, compound **11a** is more effective ($GI_{50} = 1.55$, TGI = 8.68 μM) than **8** ($GI_{50} = 58.30$, TGI = >100 μM) against the targeted leukemia RPMI-8226 cell line. Compound **8** however, reveals highly promising anti-tumor properties against SR (leukemia), SNB-75 (CNS cancer) and MALME-3M (melanoma) cell lines ($GI_{50} = 0.197$, 1.48, 0.26, TGI = 4.01, 5.34, 5.31 μM, respectively), while compound **11** exhibits highly pronounced anti-tumor properties against NCI-H226, NCI-H23 (non-small cell lung cancer), COLO 205 (colon cancer), SNB-75 (CNS cancer), OVCAR-3, SK-OV-3 (ovarian cancer), A498 (renal cancer) MDA-MB-231/ATCC and MDA-MB-468 (breast cancer) cell lines ($GI_{50} = 1.95$, 1.61, 1.38, 1.56, 1.30, 1.98, 1.18, 1.85, 1.08, TGI = 8.35, 6.01, 2.67, 8.59, 4.01, 7.01, 5.62, 6.38, 5.63 μM, respectively). It seems likely that a combination of a sulfnyl function with a chlorophenylurea residue could be a very suitable choice for designing broad spectrum anti-tumor active agents targeting various human tumor cell lines (Figs. 3 and 4).

8. Conclusions

In conclusion, the use of CODESSA PRO software provided a robust QSAR model describing the bioactivity of 34 compounds tested against the "leukemia RBMI-8226 cell line". Based on the above model, we synthesized five novel bis-urea containing-compounds, four predicted to be active and one less active. Initial anti-tumor activity results at a dose of 10 μM utilizing 55 different tumor cell lines, indicated that **11a** and **8** possess promising activity. Further screening at serial dilutions (10^{-4}–10^{-8} μM)

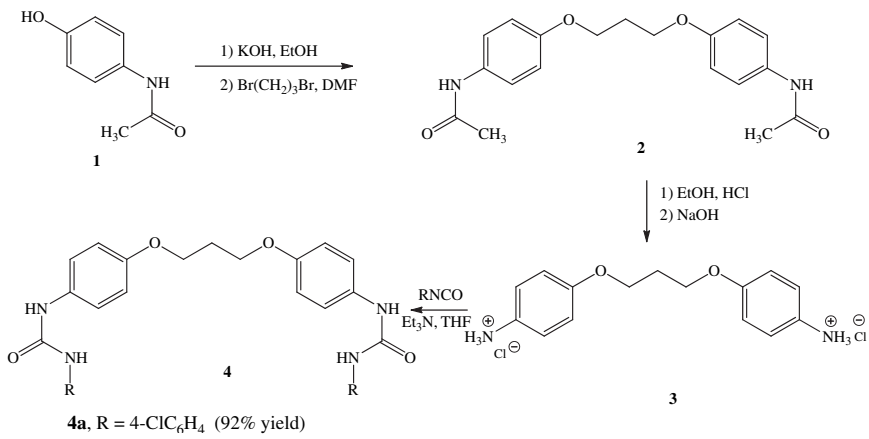

Scheme 1.

showed compound **11a** to have $GI_{50} = 1.55$, TGI = 8.68 μM, and **8** to have $GI_{50} = 58.30$, TGI = >100 μM against the targeted leukemia RPMI-8226 cell line. Compound **11a** exhibits highly pronounced anti-tumor properties against NCI-H226, NCI-H23 (non-small cell lung cancer), COLO 205 (colon cancer), SNB-75 (CNS cancer), OVCAR-3, SK-OV-3 (ovarian cancer), A498 (renal cancer) MDA-MB-231/ATCC and MDA-MB-468 (breast cancer) cell lines, suggesting that **11a** could be a lead for developing broad spectrum anti-tumor active agents.

9. Experimental section

Melting points were determined using a capillary melting point apparatus equipped with a digital thermometer and are uncorrected. ^{1}H (300 MHz) and ^{13}C (75 MHz) NMR spectra were recorded in DMSO-d_6 (with tetramethylsilane as the internal standard), unless otherwise stated. Data are reported as follows: chemical shift, multiplicity (s = singlet, d = doublet, t = triplet, q = quartet, br s = broad singlet, m = multiplet), coupling constants (*J* values) are expressed in Hz. Elemental analyses were performed on a Carlo Erba EA-1108 instrument. Anhydrous THF was obtained by distillation immediately prior to use, from sodium/benzophenone ketyl. Purity of compounds was determined by elemental analyses; purity of the target compounds was ≥95%.

9.1. Synthesis of diacetamides (*2*, *6*) (general procedure)

The appropriate acetamidophenol **1**, **5** (10 mmol) was dissolved in absolute ethanol containing KOH (10 mmol). The solvent was evaporated under reduced pressure, the residual material dissolved in DMF (10 mL) and 1,3-dibromopropane (5 mmol) was added. The mixture was heated under reflux for the appropriate time. The solvent was evaporated under reduced pressure and the residue was poured in water (100 mL). The separated solid was collected, washed with water and crystallized from a suitable solvent affording the corresponding **2**, **6**.

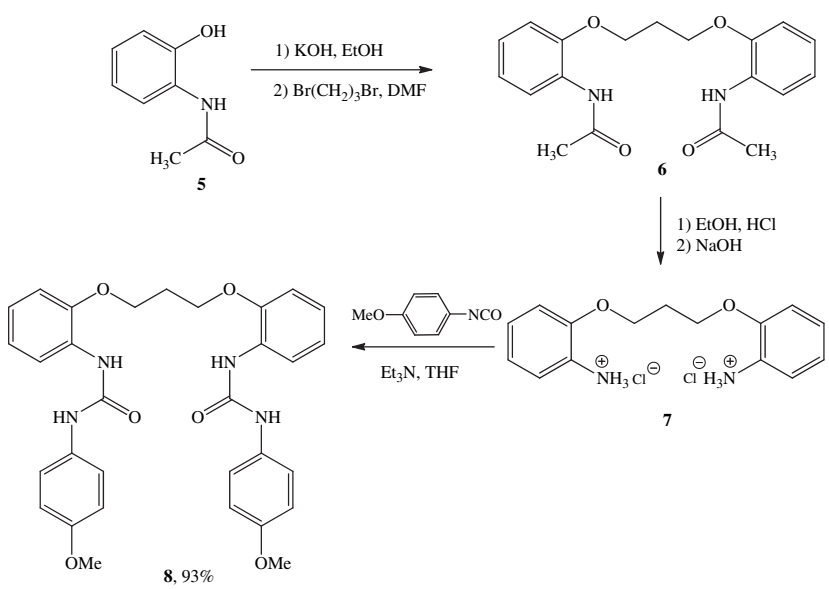

Scheme 2.

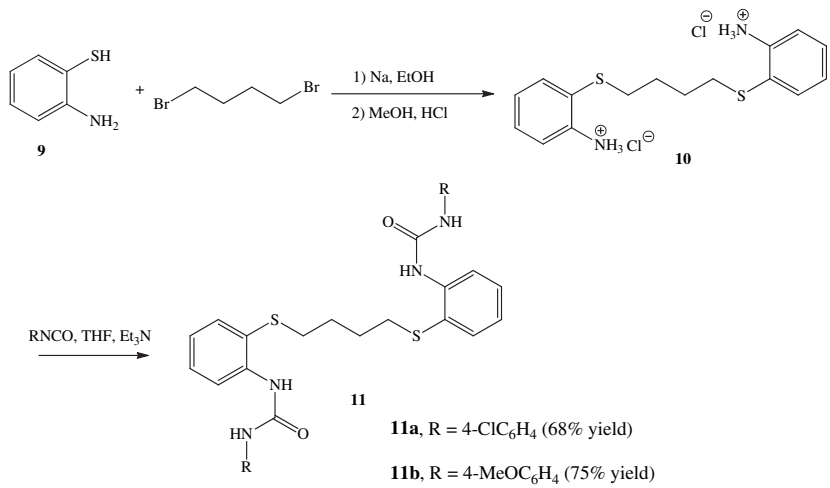

Scheme 3.

9.2. N,N′-{4,4′-[Propane-1,3-diyl(oxy)]bis(4,1-phenylene)} diacetamide (**2**)

Reaction time 1 h; colorless microcrystals from methanol; mp 178–180 °C, lit. [24] mp 191–192 °C; yield 44%. ^{1}H NMR (DMSO-d_6) δ 1.99 (s, 6H, 2 CH_3), 2.12 (quintet, $J = 6.3$ Hz, 2H, OCH_2CH_2), 4.06 (t, $J = 6.3$ Hz, 4H, 2 OCH_2), 6.87 (d, $J = 8.7$ Hz, 4H, arom. H), 7.46 (d, $J = 9.0$ Hz, 4H, arom. H), 9.78 (s, 2H, 2 NH); ^{13}C NMR (DMSO-d_6) δ 23.8 (CH_3), 28.7 (OCH_2CH_2), 64.3 (OCH_2), 114.4, 120.5, 132.6, 154.2 (arom. C), 167.7 (CO). Anal. Calcd for $C_{19}H_{22}N_2O_4$: C, 66.65; H, 6.48; N, 8.18. Found: C, 66.40; H, 6.55; N, 8.12.

9.3. N,N′-{2,2′-[Propane-1,3-diyl(oxy)]bis(2,1-phenylene)} diacetamide (**6**)

Reaction time 2 h; colorless microcrystals from ethanol; mp 192–194 °C, lit. [25] mp 193.5–194.5 °C; yield 52%. ^{1}H NMR ($CDCl_3$) δ 2.11 (s, 6H, 2 $COCH_3$), 2.30–2.42 (m, 2H, CH_2), 4.26 (t, $J = 6.0$ Hz, 4H, 2 OCH_2), 6.90–7.06 (m, 6H, arom. H), 7.73 (br s, 2H, 2 NH), 8.34 (d, $J = 7.5$ Hz, 2H, arom. H); ^{13}C NMR ($CDCl_3$) δ 25.0 (CH_3), 29.2 (CH_2), 66.1 (OCH_2), 111.6, 120.5, 121.9, 124.0, 128.2, 147.0 (arom. C), 168.4 (CO).

9.4. General procedure for the synthesis of dianilines (**3**,**7**)

A solution of the appropriate **2**, **6** (1.5 mmol) in absolute ethanol (15 mL) containing conc. HCl (4 mL) was heated under reflux for the appropriate time. The reaction mixture was poured into ice-cold water (200 mL) and made alkaline with NaOH solution (50%). The separated solid was collected washed with water and crystallized from a suitable solvent affording the corresponding **3**. In the case of **6** the dihydrochloride salt, which separated under reflux conditions was collected, washed with diethyl ether, air dried and used without further purification.

9.5. 4,4′-[Propane-1,3-diylbis(oxy)]dianiline (**3**)

Reaction time 6 h; colorless microcrystals from benzene; mp 104–106 °C, lit. [24] mp 119–121 °C; yield 65%. ^{1}H NMR ($CDCl_3$) δ 2.18 (quintet, $J = 6.3$ Hz, 2H, OCH_2CH_2), 3.41 (br s, 4H, 2 NH_2), 4.07 (t, $J = 6.3$ Hz, 4H, 2 OCH_2), 6.63 (d, $J = 8.7$ Hz, 4H, arom. H), 6.75 (d, $J = 8.7$ Hz, 4H, arom. H); ^{13}C NMR ($CDCl_3$) δ 29.8 (OCH_2CH_2), 65.5 (OCH_2), 115.9, 116.6, 140.2, 152.3 (arom. C). Anal. Calcd for $C_{15}H_{18}N_2O_2$: C, 69.74; H, 7.02; N, 10.84. Found: C, 69.96; H, 7.18; N, 10.82.

9.6. 2,2′-[Propane-1,3-diylbis(oxy)]dianiline dihydrochloride (**7**)

Reaction time 5 h; colorless microcrystals after washing with diethyl ether; mp 256–258 °C, lit. [26] mp 306–308 °C; yield 97%. ^{1}H NMR (DMSO-d_6) δ 2.25 (quintet, $J = 5.85$ Hz, 2H, CH_2), 4.35 (t, $J = 6.0$ Hz, 4H, 2 OCH_2), 7.01 (t, $J = 7.8$ Hz, 2H, arom. H), 7.25 (d, $J = 8.1$ Hz, 2H, arom. H), 7.35 (t, $J = 7.8$ Hz, 2H, arom. H), 7.48 (d, $J = 7.5$ Hz, 2H, arom. H), 10.15 (br s, 4H, 2 NH_2); ^{13}C NMR (DMSO-d_6) δ 28.3 (CH_2), 65.1 (OCH_2), 113.2, 120.7, 120.9, 123.8, 129.0, 151.5 (arom. C).

9.7. Synthesis of 2,2′-[1,4-butanediylbis(thio)]bisbenzenamine dihydrochloride (**10**)

A mixture of 2-aminothiophenol **9** (1.08 mL, 10 mmol) and 1,4-dibromobutane (0.6 mL, 5 mmol) in absolute ethanol containing sodium metal (0.23 g, 10 mmol) was heated under reflux for 2 h. After cooling, the reaction mixture was poured into ice-cold water (200 mL) and extracted with diethyl ether. The organic layer was washed with saturated sodium carbonate solution then with water and dried over anhydrous sodium sulfate, then evaporated to dryness under reduced pressure. The residue was dissolved in methanol (20 mL) and conc. HCl (37%) was added dropwise. The separated colorless crystals were collected and washed with diethyl ether affording 2,2′-[1,4-butanediylbis(thio)]bisbenzenamine dihydrochloride (**10**) in pure form, which was used without further purification (1.625 g, 86 % yield), mp 245–247 °C (lit. [27] mp 253–255 °C).

9.8. General procedure for reaction of **3**,**7** and **10** with isocyanates

A solution of the appropriate **3**, **7** or **10** (2.5 mmol) with the corresponding isocyanate (5 mmol) in dry tetrahydrofuran (10 mL) was stirred at room temperature (25 °C) for the suitable time. In the case of **7** and **10**, triethylamine (5 mmol) was added to the reaction mixture. The separated solid was collected, washed with THF to afford **4a**,**b**. In the case of **8**, **11a** the separated solid was washed with water and then with hot methanol to give colorless

Table 3
Anti-tumor properties of the tested compounds at a dose of 10 μM utilizing human tumor cell lines.

Panel/cell line	Percentage growth of tumor cell lines treated with the tested compounds				
	4a	**4b**	**8**	**11a**	**11b**
Leukemia					
CCRF-CEM	157	NT	**−7.12**	**−14.9**	75.6
HL-60(TB)	105	90.4	**18.8**	**−63.4**	120
MOLT-4	118	95.5	**-5.8**	**-6.5**	128
SR	88.7	90.4	**−39.7**	**−32.1**	143
RPMI-8226	NT	NT	77	**−4**	NT
Non-small cell lung cancer					
A549/ATCC	107	111	**−80.0**	NT	NT
EKVX	95.0	86.7	**2.2**	**-5.5**	83.1
HOP-62	96.2	95.7	**38.5**	**12.1**	84.6
HOP-92	181	81.5	NT	**−45.9**	68.1
NCI-H226	123	121	87.1	**−0.98**	85.2
NCI-H23	96.5	94.5	**2.8**	**-7.8**	88.6
NCI-H322M	102	90.2	82.4	**16.2**	90.0
NCI-H460	103	96.8	**17.7**	**10.2**	89.2
NCI-H522	91.6	98.3	63.7	**−50.8**	56.2
Colon cancer					
COLO 205	166	124	**18.6**	NT	110
HCT-116	94.8	83.3	**−36.8**	**−14.3**	72.7
HCT-15	117	118	65.5	**16.8**	99.9
HT29	114	107	54.9	**10.5**	115
KM12	110	117	**23.8**	**6.3**	89.8
SW-620	104	118	**0.7**	**13.6**	104
CNS cancer					
SF-268	125	103	50.7	**25.5**	104
SF-295	97.3	71.7	**49.0**	**−14.0**	89.4
SF-539	91.8	86.7	**−29.6**	**0.7**	86.2
SNB-19	108	94.5	**47.6**	**23.3**	86.3
SNB-75	92.2	101	**−34.8**	**10.4**	81.3
U251	103	89.8	**−50.9**	**15.9**	96.2
Melanoma					
LOX IMVI	98.1	99.3	**23.7**	**5.5**	92.9
MALME-3M	101	93.3	55.1	**3.4**	108
M14	96.7	95.5	61.4	**14.9**	88.7
MDA-MB-435	110	109	**41.6**	**6.1**	91.5
SK-MEL-2	118	108	65.8	**−51.0**	89.4
SK-MEL-28	111	204	**45.7**	**14.8**	103
SK-MEL-5	100	99.5	**48.7**	**5.5**	85.0
UACC-62	98.9	109	**3.9**	**16.5**	66.7
Ovarian cancer					
IGROV1	85.1	90.2	**4.9**	**−51.7**	49.9
OVCAR-3	112	116	**−11.4**	**-8.7**	101
OVCAR-4	110	109	**−67.2**	**17.8**	89.0
OVCAR-5	94.6	88.4	**46.0**	**12.6**	85.6
OVCAR-8	64.1	70.1	**−65.3**	NT	NT
NCI/ADR-RES	99.8	94.4	59.8	**-0.1**	80.9
SK-OV-3	122	88.4	**7.9**	NT	102
Renal cancer					
786-0	93.7	86.9	**−31.5**	**13.5**	93.8
A498	107	144	**−9.3**	**−28.0**	105
ACHN	106	100	**46.3**	**11.4**	94.0
SN12C	105	87.3	**−21.3**	**6.2**	99.8
TK-10	129	123	**22.0**	**16.1**	93.1
UO-31	68.8	71.4	**−20.7**	**−33.4**	72.1
Prostate cancer					
PC-3	93.0	108	**−36.5**	NT	NT
DU-145	121	107	**39.4**	**11.2**	104
Breast cancer					
MCF7	103	55.0	**28.2**	**4.9**	96.
MDA-MB-231/ATCC	111	93.3	**34.0**	**4.9**	88.1
HS 578T	85.4	88.2	**46.4**	**-4.8**	84.2
BT-549	102	88.1	81.2	**5.5**	83.6
T-47D	106	83.6	**9.2**	NT	90.1
MDA-MB-468	114	91.1	**22.6**	**−10.7**	76.0

NT = Not tested.

Table 4
GI_{50} and TGI values (μM) of **8** and **11a** utilizing human tumor cell lines.

Panel/Cell line	Compound **8**		Compound **11a**	
	GI_{50}	TGI	GI_{50}	TGI
Leukemia				
CCRF-CEM	14.4	78.9	2.5	>100
HL-60(TB)	26.7	68.0	2.4	7.2
K-562	31.7	>100	1.3	>100
MOLT-4	17.7	36.6	2.4	>100
RPMI-8226	58.3	>100	1.5	8.7
SR	0.2	4.0	2.23	6.5
Non-small cell lung cancer				
A549/ATCC	>100	>100	2.6	>100
EKVX	10.5	>100	2.4	>100
HOP-62	3.3	9.4	3.4	>100
HOP-92	2.7	8.6	2.0	7.1
NCI-H226	>100	>100	1.9	8.3
NCI-H23	12.4	>100	1.6	6.0
NCI-H322M	>100	>100	3.7	>100
NCI-H460	>100	>100	1.4	12.8
NCI-H522	>100	>100	1.4	>100
Colon cancer				
COLO 205	14.3	>100	1.4	2.7
HCC-2998	NT	NT	2.67	>100
HCT-116	5.3	>100	0.7	4.8
HCT-15	>100	>100	1.9	>100
HT29	>100	>100	2.6	>100
KM12	>100	>100	1.7	>100
SW-620	>100	>100	2.5	>100
CNS cancer				
SF-268	7.3	>100	2.8	>100
SF-295	29.9	>100	0.6	ND
SF-539	3.4	>100	2.1	7.3
SNB-19	4.3	26.1	1.9	>100
SNB-75	1.5	5.3	1.6	8.6
U251	3.7	28.8	2.7	>100
Melanoma				
LOX IMVI	>100	>100	2.5	>100
MALME-3M	0.3	5.3	2.5	9.4
M14	45.7	>100	2.4	>100
MDA-MB-435	>100	>100	2.6	>100
SK-MEL-2	>100	>100	2.9	>100
SK-MEL-28	>100	>100	2.5	74.1
SK-MEL-5	>100	>100	2.1	16.4
UACC-257	>100	>100	3.2	>100
UACC-62	>100	>100	NT	NT
Ovarian cancer				
IGROV1	>100	>100	3.90	>100
OVCAR-3	>100	>100	1.3	4.0
OVCAR-4	>100	>100	2.1	>100
OVCAR-5	>100	>100	2.9	>100
OVCAR-8	8.9	>100	3.3	>100
NCI/ADR-RES	>100	>100	2.2	ND
SK-OV-3	5.0	>100	2.0	7.01
Renal cancer				
786-0	ND	>100	2.8	>100
A498	16.0	72.9	1.2	5.6
ACHN	>100	>100	2.1	9.7
CAKI-1	>100	>100	1.6	>100
RXF 393	3.1	>100	3.4	>100
SN12C	>100	>100	2.6	>100
TK-10	4.0	49.7	2.8	>100
UO-31	>100	>100	2.4	>100
Prostate cancer				
PC-3	>100	>100	1.7	>100
DU-145	>100	>100	2.0	>100
Breast cancer				
MCF7	>100	>100	1.7	13.5
MDA-MB-231/ATCC	8.8	>100	1.8	6.4
HS 578T	>100	>100	1.8	14.1
BT-549	1.5	29.2	2.7	>100
T-47D	>100	>100	0.6	5.7
MDA-MB-468	NT	NT	1.1	5.6

NT = Not Tested, ND = Not Determined.

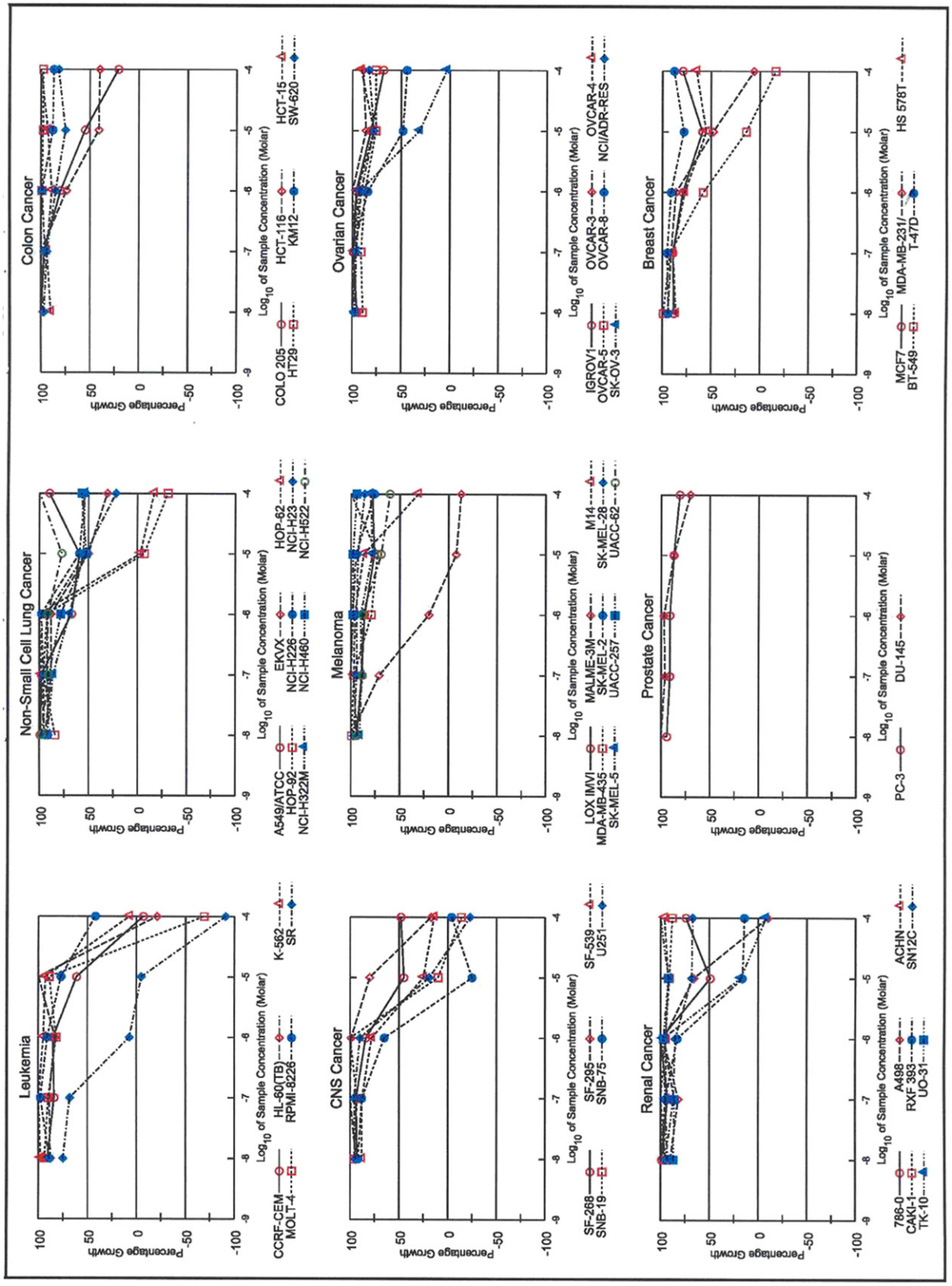

Fig. 3. Dose response curves of 1,1′-{2,2′[propane-1,3-diylbis(oxy)]bis(2,1-phenylene)}bis[3-(4-methoxyphenyl)urea] (**8**).

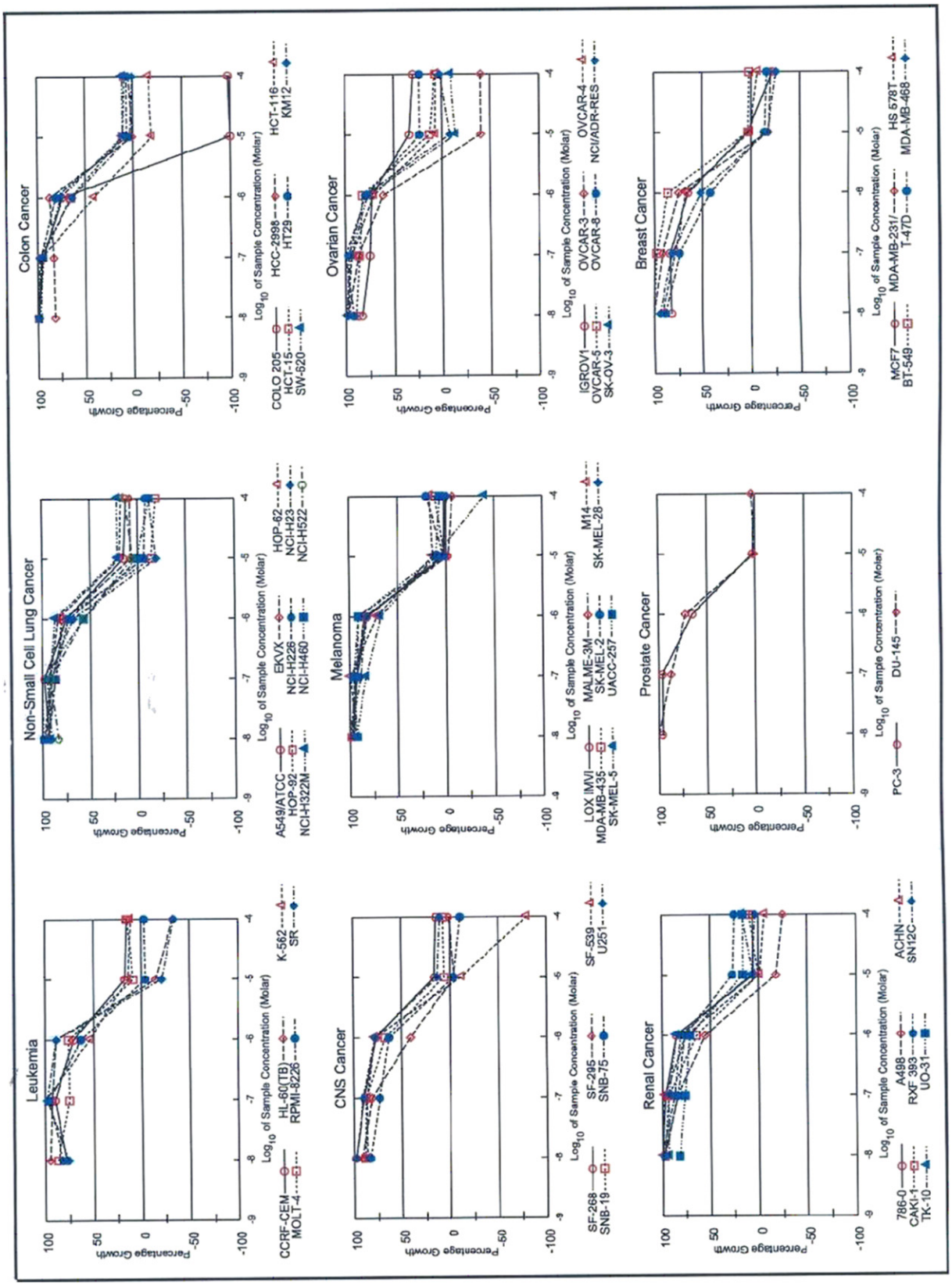

Fig. 4. Dose response curves of 1,1′-{2,2′-[butane-1,4-diylbis(sulfanediyl)]bis(2,1-phenylene)}bis[3-(4-chlorophenyl)urea] (**11a**).

microcystals, which require no further purification. In the case of **11b**, however, after washing the reaction mixture with water, it was crystallized from *n*-butanol.

9.9. 1,1′-{4,4′-[Propane-1,3-diylbis(oxy)]bis(4,1-phenylene)}bis[3-(4-chlorophenyl)urea] (**4a**)

Reaction time 3 h; colorless microcrystals after washing with tetrahydrofuran; mp 311–313 °C, yield 92%. ^{1}H NMR (DMSO-d_6) δ 2.13 (quintet, $J = 5.85$ Hz, 2H, OCH_2CH_2), 4.08 (t, $J = 6.0$ Hz, 4H, 2 OCH_2), 6.89 (d, $J = 8.7$ Hz, 4H, arom. H), 7.28–7.36 (m, 8H, arom.), 7.47 (d, $J = 8.7$ Hz, 4H, arom. H), 8.51 (s, 2H, 2 NH), 8.73 (s, 2H, 2 NH); ^{13}C NMR (DMSO-d_6) δ 28.8 (OCH_2CH_2), 64.4 (OCH_2), 114.7, 119.6, 120.1, 125.1, 128.6, 132.6, 138.9, 152.6 (arom. *C*), 153.8 (*C*O). Anal. Calcd for $C_{29}H_{26}Cl_2N_4O_4$: C, 61.60; H, 4.63; N, 9.91. Found: C, 61.57; H, 4.52; N, 9.76.

9.10. 1,1′-{4,4′[Propane-1,3-diylbis(oxy)]bis(4,1-phenylene)}bis[3-(4-methoxyphenyl)urea] (**4b**)

Reaction time 6 h; colorless microcrystals after washing with tetrahydrofuran; mp 307–309 °C; yield 89%. ^{1}H NMR (DMSO-d_6) δ 2.13 (quintet, $J = 6.15$ Hz, 2H, OCH_2CH_2), 3.71 (s, 6H, 2 OCH_3), 4.07 (t, $J = 6.15$ Hz, 4H, 2 OCH_2), 6.86 (d, $J = 8.7$ Hz, 4H, arom. H), 6.88 (d, $J = 7.8$ Hz, 4H, arom. H), 7.35 (d, $J = 9.0$ Hz, 8H, arom. H), 8.38 (s, 4H, 4 NH); ^{13}C NMR (DMSO-d_6) δ 28.8 (OCH_2CH_2), 55.1 (OCH_3), 64.4 (OCH_2), 114.0, 114.6, 119.9, 133.0, 133.1, 152.9, 153.6 (arom. *C*), 154.3 (*C*O). Anal. Calcd for $C_{31}H_{32}N_4O_6$: C, 66.89; H, 5.79; N, 10.07. Found: C, 66.94; H, 5.79; N, 9.99.

9.11. 1,1′-{2,2′[Propane-1,3-diylbis(oxy)]bis(2,1-phenylene)}bis[3-(4-methoxyphenyl)urea] (**8**)

Reaction time 24 h; colorless microcrystals after washing with methanol; mp 234–236 °C; yield 93%. ^{1}H NMR (DMSO-d_6) δ 2.34 (quintet, $J = 6.0$ Hz, 2H, CH_2), 3.71 (s, 6H, 2 OCH_3), 4.31 (t, $J = 6.0$ Hz, 4H, 2 OCH_2), 6.85–6.92 (m, 8 H, arom. H), 7.02–7.06 (m, 2H, arom. H), 7.36 (d, $J = 8.4$ Hz, 4H, arom. H), 7.98 (s, 2H, 2 NH), 8.09–8.12 (m, 2H, arom. H), 9.19 (s, 2H, arom. H); ^{13}C NMR (DMSO-d_6) δ 28.6 (CH_2), 55.2 (OCH_3), 65.1 (OCH_2), 111.7, 114.1, 118.7, 120.0, 120.6, 121.8, 129.0, 132.8, 146.8, 152.6 (arom. C), 154.5 (CO). Anal. Calcd for $C_{31}H_{32}N_4O_6$: C, 66.89; H, 5.79; N, 10.07. Found: C, 66.52, H, 5.88, N, 9.82.

9.12. 1,1′-{2,2′-[Butane-1,4-diylbis(sulfanediyl)]bis(2,1-phenylene)}bis[3-(4-chlorophenyl)urea] (**11a**)

Reaction time 48 h; colorless microcrystals; mp 210–212 °C; yield 68%. ^{1}H NMR (DMSO-d_6) δ 1.62 (br s, 4H, 2 CH_2), 2.82 (br s, 4H, 2 SCH_2), 6.98 (t, $J = 7.5$ Hz, 2 H, arom. H), 7.25 (t, $J = 7.8$ Hz, 2 H, arom. H), 7.32 (d, $J = 8.7$ Hz, 4 H, arom. H), 7.39 (d, $J = 7.8$ Hz, 2H, arom. H), 7.49 (d, $J = 8.7$ Hz, 4H, arom. H), 8.02 (d, $J = 8.1$ Hz, 2H, arom. H), 8.27 (s, 2H, 2 NH), 9.63 (s, 2H, 2 NH); ^{13}C NMR (DMSO-d_6) δ 27.5 (CH_2), 33.4 (SCH_2), 119.6, 120.6, 122.9, 123.4, 125.4, 128.1, 128.7, 133.0, 138.7, 139.4 (arom. C), 152.3 (CO). Anal. Calcd for $C_{30}H_{28}Cl_2N_4O_2S_2$: C, 58.91; H, 4.61; N, 9.16. Found: C, 58.59; H, 4.59; N, 8.98.

9.13. 1,1′-{2,2′-[Butane-1,4-diylbis(sulfanediyl)]bis(2,1-phenylene)}bis[3-(4-methoxyphenyl)urea] (**11b**)

Reaction time 24 h; mp 202–203 °C; yield 75%. ^{1}H NMR (DMSO-d_6) δ 1.62 (br s, 4H, 2 CH_2), 2.81 (br s, 4H, 2 SCH_2), 3.71 (s, 6H, 2 OCH_3), 6.87 (d, $J = 9.0$ Hz, 4H, arom. H), 6.96 (dt, $J = 1.2$, 7.5 Hz, 2 H, arom H), 7.24 (dt, $J = 1.2$, 7.5 Hz, 2 H, arom. H), 7.35–7.41 (m, 6 H, arom. H), 8.05 (d, $J = 8.1$ Hz, 2H, arom. H), 8.17 (s, 2H, 2 NH), 9.33 (s, 2H, 2 NH); ^{13}C NMR (DMSO-d_6) δ 27.5 (CH_2), 33.5 (SCH_2), 55.1 (OCH_3), 114.0, 119.9, 120.3, 122.4, 122.8, 128.1, 132.7, 133.2, 139.9, 152.5 (arom. C), 154.5 (CO). Anal. Calcd for $C_{32}H_{34}N_4O_4S_2$: C, 63.76; H, 5.69; N, 9.29. Found: C, 63.38; H, 5.96; N, 8.93.

9.14. Anti-tumor activity screening

Anti-tumor activity screening for compounds (**4a,b**; **8**, **11a,b**) at a dose of 10 μM utilizing 55 different human tumor cell lines, representing leukemia, melanoma and cancers of the lung, colon, brain, ovary, breast, prostate and kidney was carried out using adriamycin as a reference standard according to standard procedure [12–17]. The human tumor cell lines of the cancer screening panel are grown in RPMI-1640 medium containing 5% fetal bovine serum and 2 mM L-glutamine. For a typical screening experiment, cells are inoculated in 96-well-microtiter plates in 100 μL at plating densities ranging from 5000 to 40,000 cells/well depending on the doubling time of individual cell lines. After cell inoculation, the microtiter plates are incubated at 37 °C, 5% CO_2, 95% air and 100% relative humidity for 24 h prior to addition of test compounds. After 24 h, two plates of each cell lines are fixed in situ with trichloroacetic acid (TCA), to represent a measurement of the cell population for each cell line at the time of test compound addition (time zero, T_z). Tested compounds were solubilized in dimethyl sulfoxide at 400-fold the desired final maximum test concentration and stored frozen prior to use. At the time of test compound addition, an aliquot of frozen concentrate was thawed and diluted to twice the desired final maximum test concentration with complete medium containing 50 μg/mL gentamicin. Aliquots of 100 μL of the tested compound dilutions were added to the appropriate microtiter wells already containing 100 μL of medium, to give in the required final concentrations.

Following the test compound addition, the plates were incubated for an additional 48 h at 37 °C, 5% CO_2, 95% air and 100% relative humidity. For adherent cells, the assay was terminated by the addition of cold TCA. Cells were fixed in situ by the gentle addition of 50 μL of cold 50% (w/v) TCA (final concentration, 10% TCA) and incubated for 60 min at 4 °C. The supernatant was discarded, and the plates were washed five times with tap water and air dried. Sulforhodamine B (SRB) solution (100 μL) at 0.4% (w/v) in 1% acetic acid was added to each well, and plates were incubated for 10 min at room temperature. After staining, unbound dye was removed by washing five times with 1% acetic acid and the plates were air dried. Bound stain was subsequently solubilized with 10 mM trizma base, and the absorbance was read on an automated plate at 515 nm. For suspension cells, the methodology was the same except that the assay was terminated by fixing settled cells at the bottom of the wells by gently adding 50 μL of 80% TCA (final concentration, 16% TCA). Table 3 represents the observed percentage growth of each cell line treated with a test compound relative to control cell line experiments.

Due to the preliminarily nature of the observed anti-tumor properties of compounds **8** and **11a**, we screened the activity at serial dilutions (10^{-4}–10^{-8} μM), adopting the described procedure, and using the seven absorbance measurements [time zero (T_z), control growth (C) and test growth in the presence of the tested compound at the five concentration levels (T_i)], to calculate the percentage growth at each of the test compound concentration levels.

Percentage growth inhibition is calculated as $[(T_i - T_z)/(C - T_z)] \times 100$ for concentrations in which $T_i \geq T_z$, and by $[(T_i - T_z)/T_z] \times 100$ for concentrations for which $T_i < T_z$.

Growth inhibition of 50% (GI_{50}) is calculated from $[(T_i - T_z)/(C - T_z)] \times 100 = 50$, which is the test compound concentration resulting in a 50% reduction in the net protein increase (as

measured by SRB staining) in control cells during the drug incubation (Table 4).

Acknowledgment

We thank the National Cancer Institute, Bethesda, USA for anti-tumor activity screening through the Developmental Therapeutics Program. This study was supported by research grant of U.S.–Egypt Joint Board on Scientific and Technological Cooperation, grant no. MAN 10-007-002. We thank Dr. C.D. Hall for helpful discussions and a Reviewer for very helpful insightful comments and constructive criticism.

References

[1] Canadian Cancer Statistics 2005. Canadian Cancer Society – National Cancer Institute of Canada, Toronto, Canada, 2005.
[2] Canadian Cancer Statistics 2002. National Cancer Institute of Canada, Toronto, Canada, 2002.
[3] E.N. MacKay, A.H. Sellers, A statistical survey of leukemia in Ontario and at the Ontario cancer foundation clinics, 1938–1958, Can. Med. Assoc. J. 96 (1967) 1626–1635.
[4] American Cancer Society, Cancer Facts and Figures 2006. American Cancer Society, Atlanta, 2006.
[5] J. Robert, C. Jarry, Multidrug resistance reversal agents, J. Med. Chem. 46 (2003) 4805–4817.
[6] S. Hassan, S. Dhar, M. Sandstrom, D. Arsenau, M. Budnikova, I. Lokot, N. Lobanov, M.O. Karlsson, R. Larsson, E. Lindhagen, Cytotoxic activity of a new paclitaxel formulation, Pacliex, in vitro and in vivo, Cancer Chemother. Pharmacol. 44 (2005) 47–54.
[7] CODESSA PRO Software. University of Florida, 2002.www.codessa-pro.com.
[8] A.R. Katritzky, S.H. Slavov, D.A. Dobchev, M. Karelson, QSAR modeling of the antifungal activity against *Candida albicans* for a diverse set of organic compounds, Bioorg. Med. Chem. 16 (2008) 7055–7069.
[9] A.R. Katritzky, Z. Wang, S. Slavov, M. Tsikolia, D. Dobchev, N.G. Akhmedov, C.D. Hall, U.R. Bernier, G.G. Clark, K.J. Linthicum, Synthesis and bioassay of improved mosquito repellents predicted from chemical structure, Proc. Natl. Acad. Sci. 105 (2008) 7359–7364.
[10] S.C. Basak, D. Mills, Prediction of partitioning properties for environmental pollutants using mathematical structural descriptors, Arkivoc ii (2005) 60–76.
[11] A. Thakur, QSAR study on benzenesulfonamide dissociation constant pKa: physicochemical approach using surface tension, Arkivoc xiv (2005) 49–58.
[12] A.S. Girgis, H.M. Hosni, F.F. Barsoum, Novel synthesis of nicotinamide derivatives of cytotoxic properties, Bioorg. Med. Chem. 14 (2006) 4466–4476.
[13] A.S. Girgis, Regioselective synthesis of dispiro[1H-indene-2,3′-pyrrolidine-2″,3″-[3H]indole-1,2″ (1″H)-diones of potential anti-tumor properties, Eur. J. Med. Chem. 44 (2009) 91–100.
[14] A.S. Girgis, Regioselective synthesis and stereochemical structure of anti-tumor active dispiro[3H-indole-3,2′pyrrolidine-3′,3″-piperidine]-2(1H),4″-diones, Eur. J. Med. Chem. 44 (2009) 1257–1264.
[15] M.C. Alley, D.A. Scudiero, A. Monks, M.L. Hursey, M.J. Czerwinski, D.L. Fine, B.J. Abbott, J.G. Mayo, R.H. Shoemaker, M.R. Boyd, Feasibility of drug screening with panels of human tumor cell lines using a microculture tetrazolium assay, Cancer Res. 48 (1988) 589–601.
[16] M.R. Grever, S.A. Schepartz, B.A. Chabner, The National Cancer Institute: cancer drug discovery and development program, Semin. Oncol. 19 (1992) 622–638.
[17] (a) M.R. Boyd, K.D. Paull, Some practical considerations and applications of the national cancer institute in vitro anticancer drug discovery screen, Drug Dev. Res. 34 (1995) 91–109;
(b) S.X. Cai, B. Nguyen, S. Jia, J. Herich, J. Guastella, S. Reddy, B. Tseng, J. Drewe, S. Kasibhatla, Discovery of substituted *N*-phenyl nicotinamides as potent inducers of apoptosis using a cell- and caspase-based high throughput screening assay, J. Med. Chem. 46 (2003) 2474–2481.
[18] Unpublished data, Anti-tumor activity of these compounds screened through the Developmental Therapeutics Program of National Cancer Institute, Bethesda, USA and observed anti-tumor activity properties of these 24 compounds are given Table 1.
[19] ChemDraw Ultra v.11, CambridgeSoft Corporation, Cambridge, MA. www.cambridgesoft.com
[20] Hyperchem, v. 7.5, Hypercube Inc., Gainesville, FL. www.hyper.com
[21] M.J.S. Dewar, E.G. Zoebisch, E.F. Healy, J.J.P. Stewart, AM1: a new general purpose quantum mechanical molecular model, J. Am. Chem. Soc. 107 (1985) 3902–3909.
[22] (a) M. Karelson, Molecular Descriptors in QSAR/QSPR. Wiley Interscience, 2000;
(b) T. Ghafourian, M. Barzegar-Jalali, N. Hakimiha, M.T.D. Cronin, Quantitative structure–pharmacokinetic relationship modelling: apparent volume of distribution, J. Pharm. Pharmacol. 56 (2004) 339–350.
[23] L. Eriksson, J. Jaworska, A.P. Worth, M.T.D. Cronin, R.M. McDowell, P. Gramatica, Methods for reliability and uncertainty assessment and for applicability evaluations of classification- and regression-based QSARs, Environ. Health Perspect. 111 (2003) 1361–1375.
[24] P.A. Henderson, O. Niemeyer, C.T. Imrie, Methylene-linked liquid crystal dimmers, Liq. Cryst. 28 (2001) 463–472.
[25] W.A. Jacobs, M. Heidelberger, On nitro- and aminophenoxyacetic acids, J. Am. Chem. Soc. 39 (1917) 2188–2224.
[26] J.N. Ashley, R.F. Collins, M. Davis, N.E. Sirett, The chemotherapy of schistosomiasis, Part I. Derivatives and Analogues of αω-Di-(p-aminophenoxy)alkanes, J. Chem. Soc. (1958) 3298–3313.
[27] A.A. Abbas, A.S. Girgis, A convenient synthesis of thiamacrocyclic dilactams, Heteroatom. Chem. 18 (2007) 249–254.